Journal of Achievements in Materials and Manufacturing Engineering
VOLUME 37
ISSUE 2
December
2009

Phases morphology and distribution of the Al-Si-Cu alloy

K. Labisz*, M. Krupiński, L.A. Dobrzański
Division of Materials Processing Technology, Management and Computer Techniques in Materials Science, Institute of Engineering Materials and Biomaterials, Silesian University of Technology, ul. Konarskiego 18a, 44-100 Gliwice, Poland
* Corresponding author: E-mail address: krzysztof.labisz@polsl.pl

Received 10.09.2009; published in revised form 01.12.2009

Materials

ABSTRACT

Purpose: In this paper results of phase morphology investigation are presented of a newly developed Al-Si-Cu alloy. Such studies are of great interest for the metal casting industry, mainly the automotive industry, where improvement of cast elements quality is crucial for economic and quality reason and depends mainly on properly performed controlling process of the production parameters
Design/methodology/approach: The basic assumptions of this work are realised with Universal Metallurgical Simulator and Analyzer. The solidification process itself is analysed using the UMSA device using the Derivative Thermo Analysis.
Findings: During the investigation the formation of aluminium reach (α-Al) dendrites was revealed and also the occurrence of the α+β eutectic, the ternary eutectic α+Al_2Cu+β, as well as iron and manganese containing phase was confirmed. This work shows that the thermal modification of the Al-Si-Cu can be quantitatively assessed by analysis of the microstructure evaluation as well as of the cooling curve thermal characteristics.
Research limitations/implications: The investigations were performed using standard metallographic investigation as optical, scanning and transmission electron microscopy methods; also the EBSD phase identification method based on the kikuchi lines identification was used. The results in this paper are valuable only for the Al_2Cu, Fe and Mg containing phases, and are not performed for the assessment of the Silicon Modification Level.
Practical implications: As an effect of this study it will be possible to understand and to influence the mechanism of structure forming, refinement and nucleation. Also better understanding of the thermal characteristics will be provided to achieve a desirable phase morphology required for specific application of this material under production conditions.
Originality/value: The originality of this work is based on applying of regulated cooling rate of aluminium alloy for structure and mechanical properties changes. In this work the dependence among the regulated cooling speed, chemical composition and structure of the investigated aluminium cast alloy on the basis of the thermo-analysis was presented.
Keywords: Metallic alloys; Electron microscopy; Thermo analysis; Phases morphology; Aluminium

Reference to this paper should be given in the following way:
K. Labisz, M. Krupiński, L.A. Dobrzański, Phases morphology and distribution of the Al-Si-Cu alloy, Journal of Achievements in Materials and Manufacturing Engineering 37/2 (2009) 309-316.

1. Introduction

In the recent years together with development of the car industry and desire for lowering the energy consumption of production processes, tendencies have appeared to return to casting alloys in sand moulds made on highly efficient automatic lines. Newly developed technologies ensure filling the sand moulds under elevated pressure and reduce oxidation of the applied aluminium alloys. The usage of highly efficient automatic cast lines made it necessary to work out a fast, cheap and precise estimation method for the quality of cast alloys. Properly chosen technological factors have influence on the crystallization kinetics of the aluminium alloys, involving such elements like the mould diameter, as well the casting temperature which decreases together with the crystallization rate of the castings and the alloy overcooling grade, this causes in this way a prolongation of the crystallization time [1, 2].

The W319 aluminium alloy was successfully used in the automotive industry as material for engine blocks and cylinder heads. In order to improve the mechanical properties of these components they are often heat treated using a two-step process (i.e. solution treatment and artificial aging). Two important solution treatment process variables are time and temperature. They are responsible for Si phase modification and for the dissolution of Cu- and Mg-enriched phases [3, 4].

The novel universal metallurgical simulator and analyzer (UMSA) (Fig. 1) technology platform is capable of collecting in situ and analyzing on-line, the thermal characteristics of metallurgical treated melts and solidifying the heat-treated test samples, using precision-controlled heating and cooling rates while simulating industrial conditions [5-12].

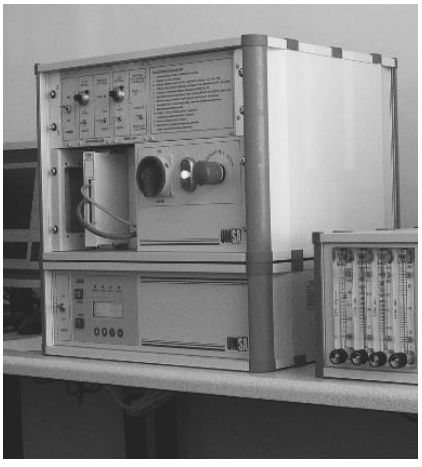

Fig. 1. UMSA device generator used for the thermal derivative analysis with gas flow control unit for regulated quenching and inert gas input.

For determination and calculation of the thermal processes parameters occurring during the solidification, some thermodynamical calculations should be performed. A very important tool is the cooling rate curve with determined baseline. The baseline equation calculation requires the thermal system being considered (i.e., alloy sample and cup) complies with Newtonian cooling model requirements. This means that the temperature within the system must be spatially uniform or, at least, that the temperature gradient in any direction within the system must be negligible at any instant during the cooling process.

The overall heat transmission coefficient is based on the total thermal resistance between the temperature of the solidifying sample (T_c) and the ambient temperature (T_∞).

Under the described assumption, the energy balance can be written as follows:

$$\rho C_\rho V \frac{d(T_c - T_\infty)}{dT} = -UA(T_c - T_\infty) + \frac{dQ_L}{dt} \quad (1)$$

In case, where no metallurgical reaction occurs (i.e., when $Q_L = 0$) equation 1 can be reduced to another form, where the baseline equation can be set:

$$\frac{dT_c}{dt} = \left(-\frac{UA}{\rho C_\rho V} \right)(T_c - T_\infty) \quad (2)$$

where:

Q_L - Crystallisation heat *Cp* - Heat capacity, U – heat transmission coefficient, dT_c/dt - *D*ifferential, *dt*, T_O Ambient temperature, T_c – *S*olidification point, $\rho C_\rho V$ – Heat capacity term

However, since this new alloy was recently engineered, the solidification kinetics and the sequence of the phase transformations in relation to the as-cast and heat-treated structures need to be further understood, quantified and implemented for further improvement of the casting technology and cast component service characteristics. Moreover, the optimum conditions for liquid metal treatment must be understood to gain full benefit from the achievable refinement of the primary Si particles. The cooling rate is proportional to the heat extraction from the sample during solidification. Due to the increase, the cooling rate, the nucleation undercooling increase. The phenomenon of increase in the nucleation temperature with increase in the solidification rate depends on mobility of clusters of atoms in the melt. These groups of the frozen atoms produce fluctuation clusters and fluctuation embryos which are the nucleation primers. The increase of the cooling rate with increased amount of the nucleation primers and reduction of the recalescence temperature is a well established fact. This effect has influence on the grain size, precipitation morphology and distribution [13-19].

The concept of this work include rapid and slow quenching rate experiments to monitor the solidification process mainly of the Al_2Cu iron and magnesium containing phases. The goal of this paper is to present the structure changing mechanism on the basis of the characteristics of the Al-Si-Cu alloy which is widely used for monolithic engine block in the automotive industry due to its good casting characteristics and mechanical properties.

High purity Al-Si-Cu hypoeutectic alloys exhibit three main solidification reactions during the solidification process, starting with the formation of aluminum dendrites followed by the

development of two main eutectic phases. The presence of alloying and impurity elements such as Cu, Mg, Mn and Fe leads to more complex constituents (including intermetallic) that are characterised by metallographic techniques. Bäckerud et al. identified the reactions in (3XX.X) alloys and listed the solid-state phases which can be described in the following way as the solidification path for the investigated alloy:

- Nucleation of α-Al dendrite network (liquidus temperature ca. 602 ºC). The exact temperature value mainly depends on the Si and Cu concentration in the alloy.
- Liq. → Al + Al_{15} (Fe, Mn)$_3Si_2$ ca. 590 ºC, (Bäckerud reports also the occurrence of a $Al_{15}Mn_3Si_2$ phase, which was not detected during the investigation).
- Liq. → Al + Si + Al_5FeSi phase within the range of 575–507 ºC, leading to a further localized increase in Cu content of the remaining liquid.
- Liq. → Al + Al_2Cu + Al_5FeSi + Si, reduction of temperature allows nucleation of Cu-enriched eutectic (Al+Al_2Cu) between 525 and 507 ºC.
- Liq. → Al + Si + Al_2Cu + $Al_5Mg_8Cu_2Si_6$ at 507 ºC
- End of the alloy solidification (solidus temperature) ca. 483 ºC.

According to the literature study, the following phases can be expected in this aluminium cast alloy grade: α-Al, $Al_{15}Mn_3Si_2$, Al_5FeSi, $Al_5Mg_8Cu_2Si$, Al_2Cu, Si and Cu_2Al [20-25].

In this paper, there are presented especially the effect of cooling rate on the size and distribution of the precipitation occurred in the matrix and thermal characteristic results of this AC-AlSi7Cu3Mg grade aluminium cast alloy. It was observed when the cooling rate/ solidification rate increases the precipitations, mainly the Al_2Cu phases size decreases and higher homogenous distribution in the matrix can be obtained. Similarly, the process occurs for the iron and magnesium containing phases. The thermal analysis was performed at low but regulated cooling rate in the range of 0.2 ºC – 1.25 ºC. Cooling curve for the thermal analysis was performed using high sensitivity thermocouples of the K type, covered with a stainless steel sheath. The data were acquired by a high speed data acquisition system linked to a PC computer. Two different types of samples were used: bulk-cylindrical and thin-walled cylindrical. Metallographic investigation was made on cross section samples of an engine block. Non-equilibrium heating and cooling process conditions were applied to achieve changes in the shape and distribution of the phases such as Al_2Cu and Si.

2. Experimental conditions

2.1. Material for investigation

The experimental alloy used in this investigation was the W319 aluminium grade cast alloy with chemical composition showed in table 1. The material used for investigation has been supplied in a form of cut parts of a block engine. The alloy was heat treated according to the standard steps for this aluminium grade – a properly chosen solution for heat treatment and ageing.

Table 1.
Chemical composition of AC-AlSi7Cu3Mg aluminum cast alloy according to the PN-EN 1706:2001 used for investigation

Mass concentration of the element, in wt. %, AA standard			
Si	Cu	Mg	Mn
6.5-8	3-4	0.3-0.6	0.2-0.65
Fe	Ti	Zn	Ni
≤ 0.8	≤ 0.25	≤ 0.65	≤ 0.3
Mass concentration of the element, in wt. %, Actual sample			
Si	Cu	Mg	Mn
7-7.8	3.3-3.7	0.25-0.35	0.2-0.3
Fe	Ti	Zn	Ni
≤ 0.4	0.1-0.15	≤ 0.25	≤ 0.1

The experimental alloy used in this investigation was the W319 aluminium grade cast alloy with chemical composition showed in Table 1. The material used for investigation has been supplied in a form of cut parts of a block engine. The alloy was heat treated according to the standard steps for this aluminium grade – a properly chosen solution for heat treatment and ageing.

2.2. Thermal analysis using the UMSA analyser

For performing of the thermal analysis and solidification process, the UMSA device was used with low-density ceramic crucibles for improving the thermal inertia of the system. For temperature measurement a chromel-alumel thermocouple was applied. The cooling rate was set experimentally to low = 0.2 ºC/s, middle = 1 ºC/s and high = 1.25 ºC/s.

The solidification process itself was performed without any protective atmosphere in the open air environment to achieve a maximum cooling rate, the compressed air quenching gas was used with the gas flow rate of 20 l/min through a circular nozzle with diameter of 12 mm, the pressure was set to 8 ATM and held at this level. After the experiments conditions setting, the samples were preheated to 750 ºC and held for 300 s.

2.3. Investigation methods

After the heat treatment, the samples surfaces were ground on a magnetic grinding machine. Special care was taken to avoid micro cracks and scratches which can disqualify the sample on future investigation. Operation parameters for this experiment are presented in Table 2. Samples of this material were in the form of plate, of rectangular shape with dimensions 15 x 15 x 5 mm. The UMSA test analysis samples were cut longitudinally, and then, sectioned horizontally approximately 15 mm from the bottom and were prepared for metallographic analysis using standard procedures.

For surface preparation, the standard metallographic procedure was applied in the form of grinding using SiC 220, 500, 800 and 1200, polishing with 1µm diamond and 0,04 µm SiC polishing paste and drying, the samples were mounted in the thermo hardened resin supplied by Struers. Next, the samples were etched in 5% HF solution at room temperature for the experimentally chosen time of 25 s for phases etching. For structure etching, the main recommended solution is a NaOH agent.

Table 2.
Operation parameters

Parameter	Value
Maximum heating temperature ºC	750
Quenching gas flow, l/min	20
Relaxation time, s	60

Structure investigation was performed using the light microscope Leica MEF4A supplied by Zeiss in the magnification range of 50 - 100x. The micrographs of the microstructures were made by means of the KS 300 program using the digital camera.

The observations were performed on the vertical and horizontal cross section of the sample. Metallographic investigations were performed also using the Zeiss Supra scanning electron microscope supplied by ZEISS in the magnification range of 500 - 15000x. Hardness measurements results were registered for each remelting area, for this reason the Rockwell hardness tester TK 4150 supplied by Zwick was used according to the PN-EN ISO 6507-1 standard with the HRF scale.

3. Experimental conditions

3.1. Material for investigation

Investigation performed using the optical microscope reveal the microstructure of the investigated cast aluminium alloy; the optical micrographs of samples cooled with different cooling rate are presented in Figures 2 and 3. In each of the figures the three main phases, occurred in the alloy, can be discovered. One of them is the primary silicon Si phase. Etched with HF acid the Si phase is coloured dark gray and appears in the shape of very irregular, longitudinal sharp-edged and fuzzy structures. On the basis of the made investigation it can be stated that this phase consists only of the primary Si precipitation because the maximal heating temperature in the UMSA device was set to 750 °C, and this value is too low to solute the Si phase in the melt. The next described phase also well known in the literature is the Al_2Cu phase. This phase appears light gray in the etched optical micrographs for every applied cooling rate; the precipitation is longitudinally shaped with eutectic-like structure. This phase is also present across the whole structure.

On the basis of the investigation made, also iron and manganese containing phase is confirmed, some results achieved using EBSD analysis give the Al_{17} (Fe, Mn)$_4Si_2$ or more exactly $Al_{17}(Fe_{3,2}Mn_{0,8})Si_2$ formula as a possible solution. An important discovered feature is that the Al_2Cu and iron/manganese containing phase seems to be not uniformly distributed and shows some areas that are etched black. Investigation using scanning electron microscope and EDS analysis can help to solute this problem.

3.2. Scanning and transmission electron microscope investigation and EDS microanalysis

As a result of TEM investigation a bright and dark field image, as well as diffraction pattern of the Al_2Cu phase and Al matrix are presented in Figures 8-10. As a result of SEM investigation - iron and manganese containing phase (Fig. 11), Si phase (Fig. 12) as well as Al matrix with Cu and Mg containing phases (Fig. 13) are presented. EDS microanalysis (Figs. 4, 5, 6, 14, 15, 16) on the scanning electron microscope was used to identify the chemical composition of the phases present in the alloy. In figure 13 there is a presented, not identified magnesium containing phase, Bäckerund gives the Mg_2Si phase as a possible solution.

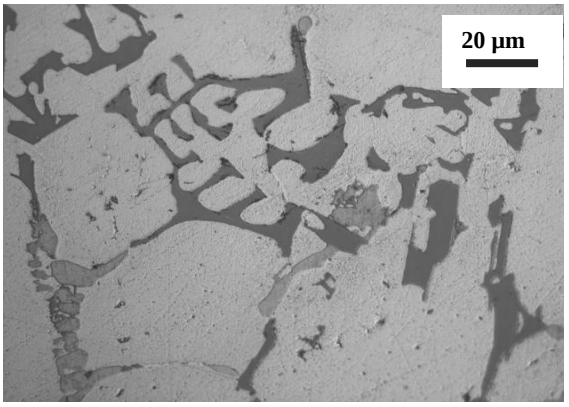

Fig. 2. Microstructure of the aluminium alloy remelted at a slow cooling rate

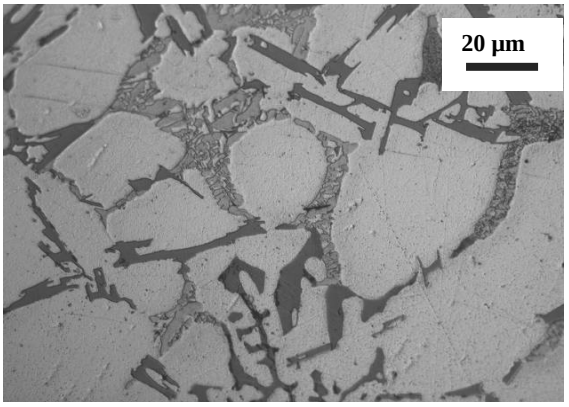

Fig. 3. Microstructure of the aluminium alloy remelted at a medium cooling rate

3.3. Mechanical properties

The hardness was measured by the Rockwell hardness tester, primarily by the HRF scale with a load of 60 kg and converted automatically into the HB scale. A minimum of 10 indentations was made on each of the heat treated samples.

Mechanical properties (Fig. 7) of the aluminum alloys are strongly dependent on the effect of applied cooling rate. Investigations results show that increase of the cooling rate increases the achieved hardness value. For the lowest cooling rate, the obtained hardness was 69 HB and increase to 75 HB for a medium cooling rate. For the highest applied cooling rate, the hardness value reaches a value of 92 HB.

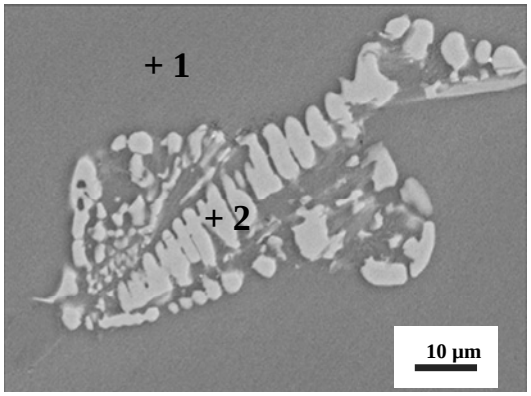

Fig. 4. SEM micrograph of the Al_2Cu phase

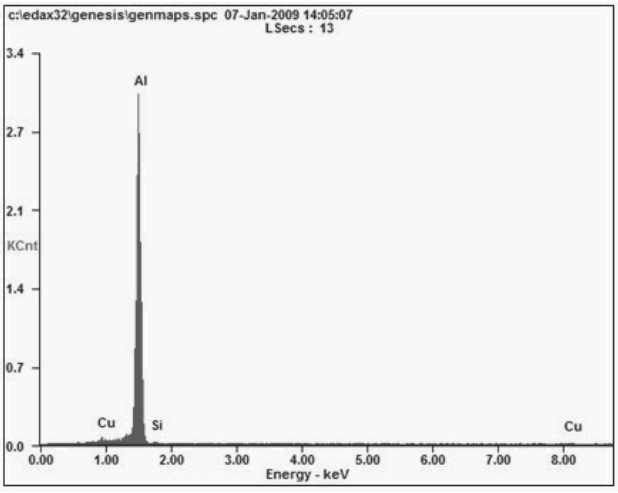

Fig. 5. EDS point wise analysis of the investigated aluminium cast alloy, marker 1 in Figure 4

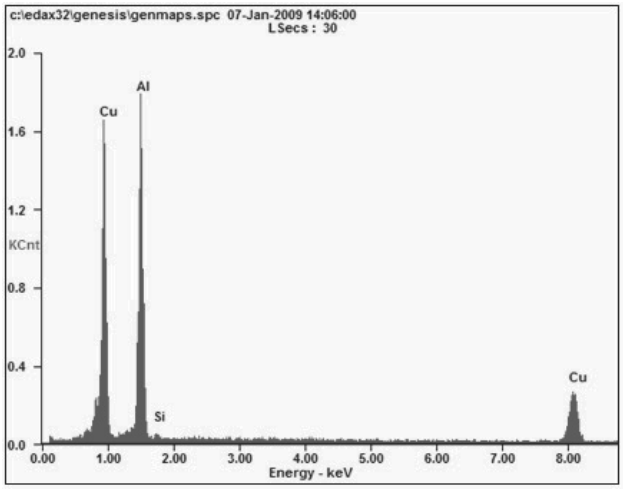

Fig. 6. EDS point wise analysis of the investigated aluminium cast alloy, marker 2 in Figure 4

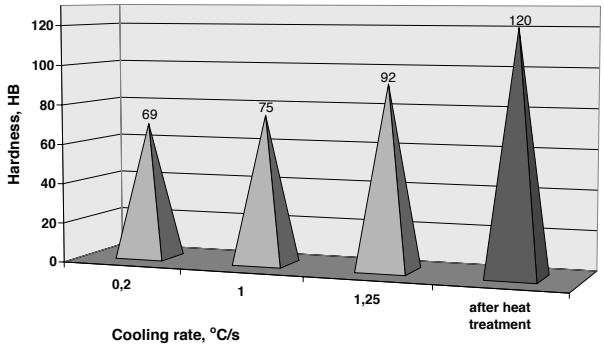

Fig. 7. Hardness measurement results

a)

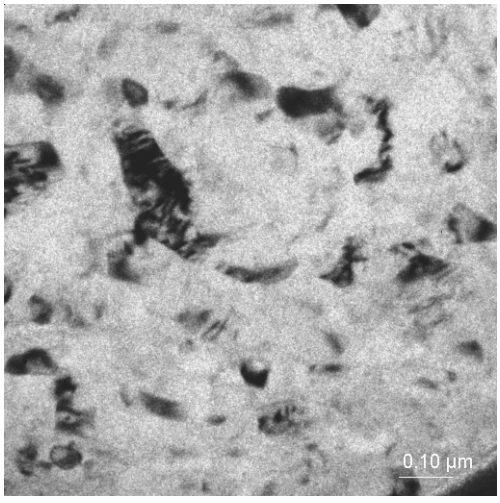

b)

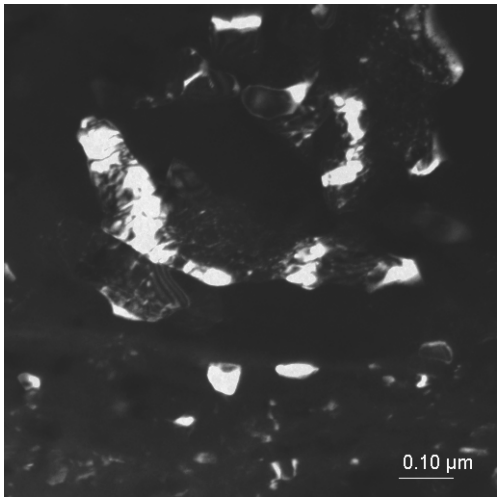

Fig. 8. Thin foil structure of the investigated alloy, a) bright field image, b) dark field image, TEM

a)

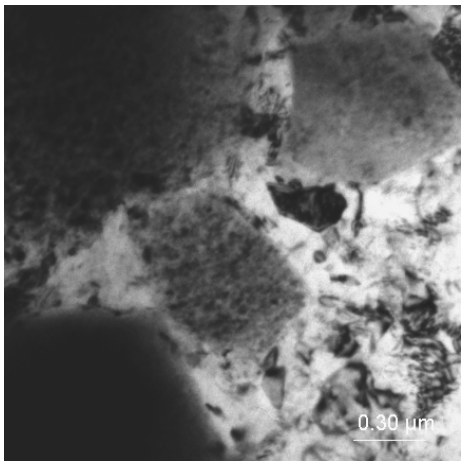

b)

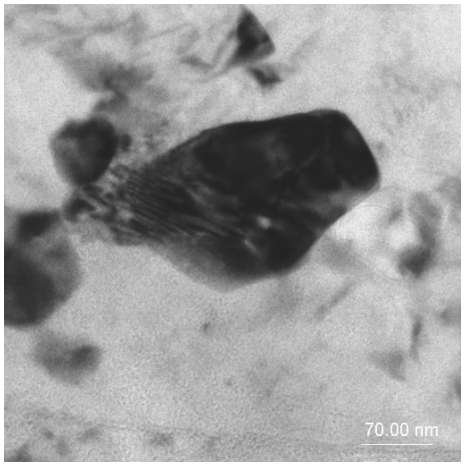

c)

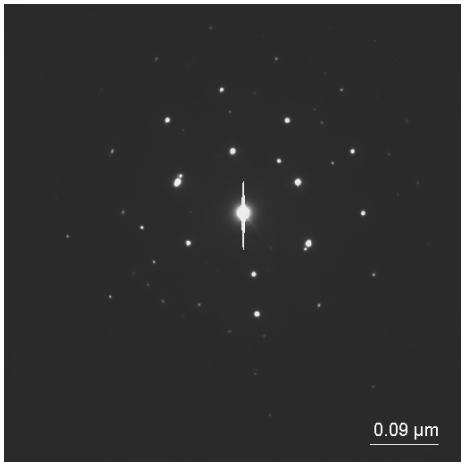

Fig. 9. Thin foil structure of the investigated alloy, a) bright field image of the Al-matrix, b) bright field image of the Al_2Cu phase, TEM diffraction pattern of the area in fig. b

a)

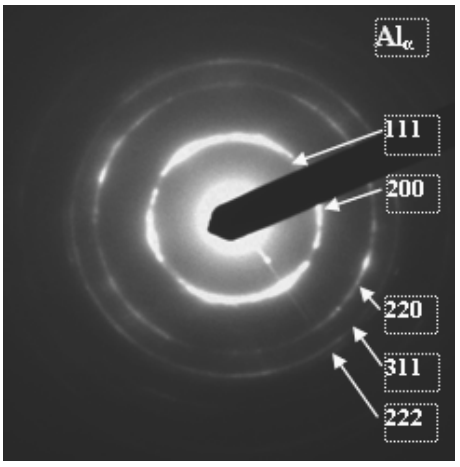

b)

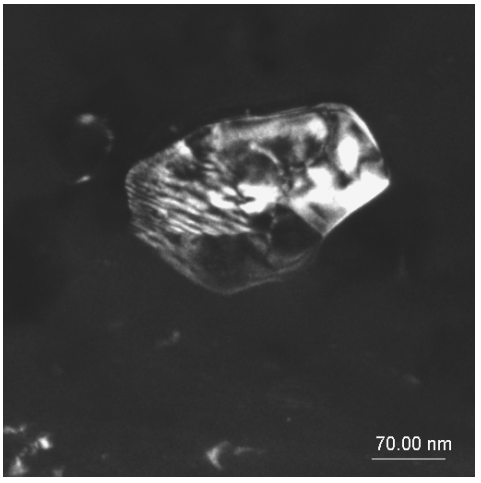

c)

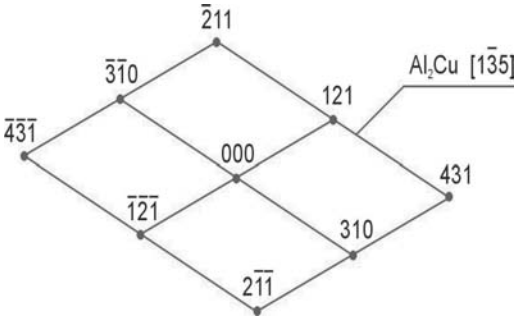

Fig. 10. TEM diffraction pattern of the area in fig. 9a, dark field image of the area in fig. 9b, diffraction pattern solution of the diffractogram in Fig. 9c, TEM

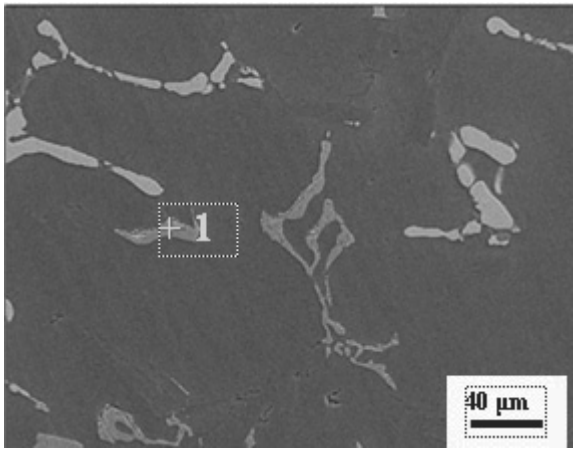

Fig. 11. SEM micrograph of the iron and manganese containing phase of the investigated aluminium alloy

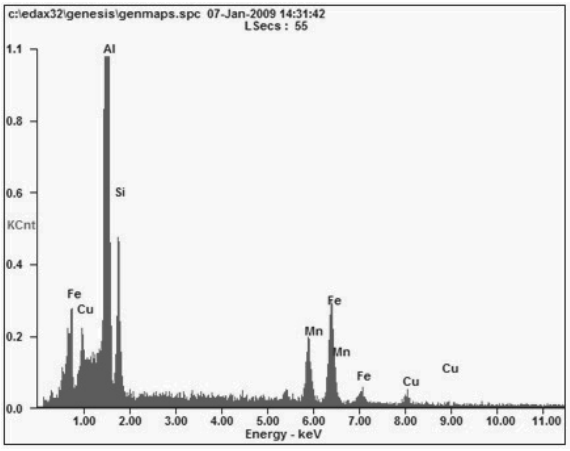

Fig. 14. EDS point wise analysis of the investigated aluminium cast alloy, marker 1 in Figure 11

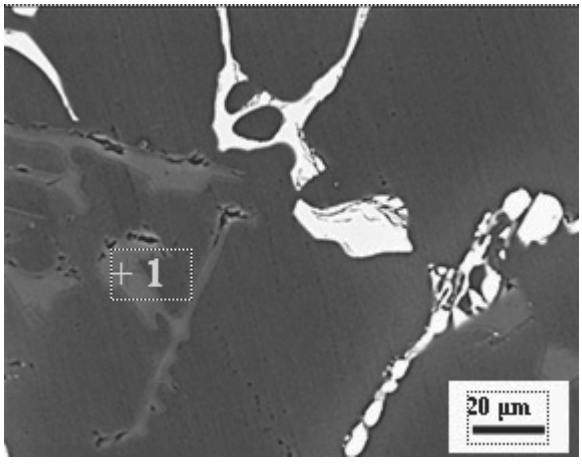

Fig. 12. SEM micrograph of the silicon phase – gray coloured

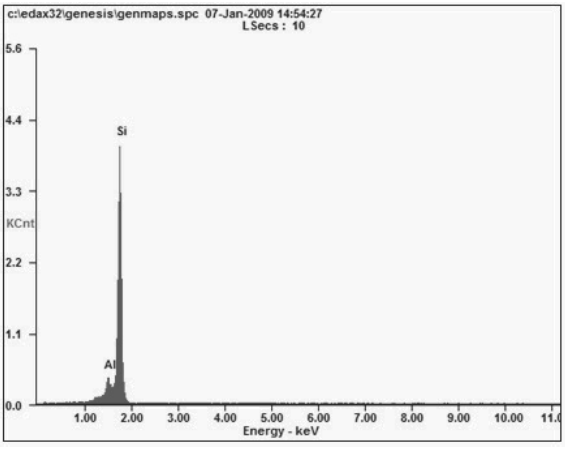

Fig. 15. EDS point wise analysis of the investigated aluminium cast alloy, marker 1 in Figure 12

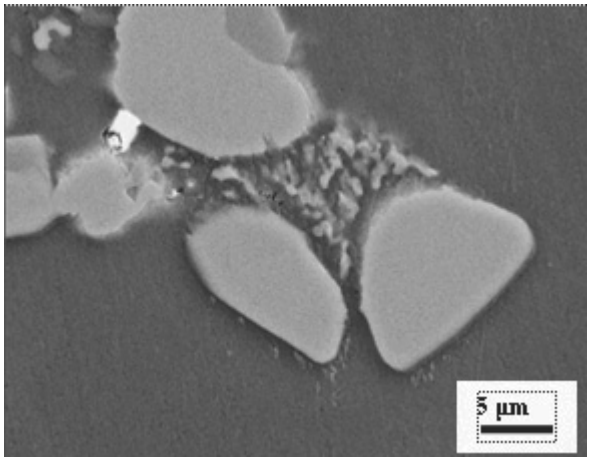

Fig. 13. SEM micrograph of the unknown magnesium containing phase of the investigated aluminium alloy

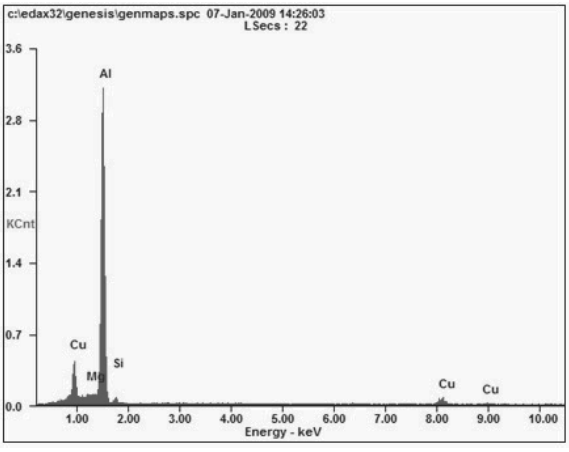

Fig. 16. EDS point wise analysis of the investigated aluminium cast alloy, performed of the whole area presented in Figure 13

4. Conclusions

On the basis of the performed investigations the following conclusions can be stated:

- Solidification condition, particularly affected by the cooling rate influences the morphology of the phases occurred in the investigated Al alloy. With increasing cooling rate, the size of the phases decreases, and the distribution is more homogeneous, because of an increased nuclei number that affect the number, and thus, size of the precipitations.
- Three different types of phases are confirmed in this alloy, these are the primary silicon phase, the Al_2Cu (confirmed by TEM diffraction method) and, manganese and iron containing phase identified using the EBSD analysis as $Al_{17}(MnFe)_4Si_2$ phase.
- Generally, structure and phase refinement can be relocated to the chosen cooling rate.

References

[1] M. Krupiński, L.A. Dobrzański, J.H. Sokołowski: Microstructure analysis of the automotive Al-Si-Cu castings, Archives of Foundry Engineering 8 (2008) 71-74.

[2] L.A. Dobrzański, M. Krupiński, K. Labisz, Derivative thermo analysis of the near eutectic Al-Si-Cu alloy, Archives of Foundry Engineering 8/4 (2008) 37-40

[3] H. Yamagata, H. Kurita. M. Aniolek, W. Kasprzak, J.H. Sokołowski, Thermal and metallographic characteristics of the Al-20% Si high-pressure die-casting alloy for monolithic cylinder blocks, Journal of Materials Processing Technology 199 (2008) 84-90.

[4] X. Chen, W. Kasprzak, J.H. Sokołowski: Reduction of the heat treatment process for Al-based alloys by utilization of heat from the solidification process, Journal of Materials Processing Technology 176 (2006) 24-31.

[5] L.A. Dobrzanski, R. Maniara, J. Sokołowski, W. Kasprzak: Effect of cooling rate on the solidification behaviour of AC AlSi7Cu2 alloy, Journal of Materials Processing Technology 191 (2007) 317–320.

[6] J.G. Kauffman, E. L. Rooy, Aluminum Alloy Castings, ASM International, Ohio 2005.

[7] S.G. Shabestari, M. Malekan, Thermal Analysis Study of the Effect of the Cooling Rate on the Microstructure and Solidification Parameters Of 319 Aluminum Alloy, Canadian Metallurgical Quarterly, 44, 2005.

[8] L.A Dobrzański, K. Labisz, R. Maniara, Microstructure investigation and hardness measurement in Al-Ti alloy with additions of Mg after heat treatment, Proceedings of the 13th International Scientific Conference COMMENT 2005, Gliwice-Wisła, 2005.

[9] L. Bäckerud, E. Król, J. Tamminen: Solidification Characteristics of Aluminum Alloys, Vol. 1, Universitetsforlaget, Oslo, 1986.

[10] L. Bäckerud, G. Chai, J. Tamminen, Solidification Characteristics of Aluminum Alloys 2, AFS, 1992.

[11] L. Bäckerud, G. Chai: Solidification Characteristics of Aluminum Alloys 3, AFS, 1992.

[12] Ł. Bernat, J. Hajkowski, M. Hajkowski: Microstructure and porosity of aluminum alloy casting whereas mechanical properties, Archives of Foundry 6/22 (2006) 41-48 (in Polish).

[13] L.A. Dobrzański, R. Maniara, J.H. Sokolowski: The effect of cast Al-Si-Cu alloy solidification rate on alloy thermal characteristics, Journal of Achievements in Materials and Manufacturing Engineering 17 (2006) 217-220.

[14] A. Fajkiel, P. Dudek, G. Sęk-Sas, Foundry engineering XXI c. Directions of metallurgy development and Ligot alloys casting, Publishers Institute of Foundry Engineering, Cracow, 2002.

[15] P.D. Lee, A. Chirazi, R.C. Atwood, W. Wan, Multiscale modelling of solidification microstructures, including microsegregation and microporosity, in an Al–Si–Cu alloy, Materials Science and Engineering A365 (2004) 57–65.

[16] M. Krupinski, L.A. Dobrzański, J.H. Sokolowski, W. Kasprzak, G. Byczynski, Methodology for automatic control of automotive Al-Si cast components, Materials Science Forum 539-543 (2007) 339-344.

[17] C.H. Caceres, M.B. Djurdjevic, T.J. Stockwell, J.H. Sokolowski, The effect of Cu content on the level of microporosity in Al-Si-Cu-Mg casting alloys, Scripta Materialia 40 (1999) 631–637.

[18] R. MacKay, M. Djurdjevic, J. H. Sokolowski, The Effect of Cooling Rate on the Fraction Solid of the Metallurgical Reaction in the 319 Alloy, AFS Transaction, 2000.

[19] C. H Cáceres, M. B. Djurdjevic, T. J. Stockwell, J. H. Sokolowski, Cast Al: The Effect of Cu Content on the Level of Microporosity in Al-Si-Cu-Mg Casting Alloys, Scripta Materiala, 1999.

[20] E. Carrera, A. Rodriguez, J. Talamantes, S. Valtierra, R. Colas, Measurement of residual stresses in cast aluminium engine blocks, Journal of Materials Processing Technology 189 (2007) 206-210.

[21] L.A. Dobrzański, M. Krupiński, J.H. Sokolowski, Application of artificial intelligence methods for classification of defects of Al-Si-Cu alloys castings, Archives of Foundry 6/22 (2006) 598-605 (in Polish).

[22] Z. Muzaffer: Effect of copper and silicon content on mechanical properties in Al–Cu–Si–Mg alloys, Journal of Materials Processing Technology 169 (2005) 292–298.

[23] D. Ovono, I. Guillot, D. Massinon, The microstructure and precipitation kinetics of a cast aluminium alloy, Scripta Materialia 55 (2006) 259–262.

[24] G. Mrówka-Nowotnik, Damage mechanism in AlSi1MgMn alloy, Archives of Materials Science and Engineering 29/2 (2008) 93-96.

[25] S. Rusz, K. Malanik, Refining of structure of the alloy AlMn1Cu with use of multiple severe plastic deformation, Journal of Achievements in Materials and Manufacturing Engineering 27/2 (2008) 167-178.